INDIAN JOURNAL OF SCIENCE AND TECHNOLOGY

RESEARCH ARTICLE

Enhancement of the tribological performance of pure titanium (CP-Ti) through YAG laser technique

Essam R I Mahmoud[1,2]*

1 Department of Mechanical Engineering, Faculty of Engineering, Islamic University of Madinah, 41411, Saudi Arabia
2 Central Metallurgical Research and Development Institute, Cairo, 11421, Egypt

OPEN ACCESS

Received: 13.10.2020
Accepted: 13.12.2020
Published: 19.12.2020

Citation: Mahmoud ERI (2020) Enhancement of the tribological performance of pure titanium (CP-Ti) through YAG laser technique. Indian Journal of Science and Technology 13(46): 4555-4563. https://doi.org/10.17485/IJST/v13i46.1858

* **Corresponding author**.

Essamibrahim2@yahoo.com

Funding: Scientific Research Deanship, Islamic University of Madinah, with Tamayyuz grant number 7/40

Competing Interests: None

Published By Indian Society for Education and Environment (iSee)

ISSN
Print: 0974-6846
Electronic: 0974-5645

Abstract

Background/Objectives: The poor wear resistance of pure titanium has significantly limited its industrial and biomedical applications, especially when it is used in severe conditions. To overcome this limitation, surface treatment must be done to improve the wear resistance without negatively affect its excellent corrosion resistance. **Methods:** To prepare titanium for use under severe wear and friction conditions, its surfaces were laser melted using YAG Fiber laser at powers of 1000, 1500 and 2000 W, and travelling speeds of 4 and 30 mm/s. The processes were conducted in argon atmosphere. **Findings:** In all cases, three zones were observed: melted zone, heat-affected zone and base metal. The increase of the power and/or decrease of the travelling speed caused increases in the depths of the melted zones. Acicular martensite α' structure was observed within the melted and solidified zone. A hardened surface layer of 445 HV with improvement of 62%, with reference to CP-Ti base metal, was produced by application of the treatment at power of 1000 W and travelling speed of 4 mm/s. When the travelling speed with increased to 30 mm/s, the surface hardness reached 710 HV. The depth of hardened layer was increased from nearly 0.6 mm to 0.8 mm by increasing processing power from 1000 W to 2000 W at travelling speed of 4 mm/s. Remarkable improvements in wear and corrosion resistances of the treated specimens were achieved. The weight losses of the un-treated substrate were almost 5 times (2.4 gm) of the laser treated sample at 1500 W and 30 mm/s (0.5 gm). For corrosion, the corrosion potentials were shifted to more positive values and the corrosion current was shifted to more negative values for the laser treated sample at 1000 W compared to the un-treated sample. **Applications:** the findings will widen the application of pure titanium in many biomedical and industrial fields.

Keywords: Commercially pure titanium; surface microhardness; wear resistance; corrosion resistance; laser surface melting

1 Introduction

Titanium alloys are extensively used in wide range of applications such as biomedical, automotive and aircraft industries [1–4], marine and chemical industries due to their low density, high weight-to-strength ratio, excellent resistance for corrosion, oxidation and high-temperature [2–5]. Among titanium alloys, pure titanium (Ti) has excellent corrosion resistance against most of corrosive media. Also, pure Ti is more biocompatible with human fluids and tissue than other materials [6]. At the same time, pure titanium has a low elastic modulus, which is similar to that of cortical bone, which considers it a good candidate for orthopedic implants [7]. However, the application of pure titanium, especially for the coarse-grained titanium, under severe wear and friction conditions is highly restricted due to their poor tribological properties [2]. In addition, the most failures in pure titanium that are used in medical implants are wear and fatigue. For that reason, pure titanium could leave metal debris in the tissue in fretting conditions [8]. In addition, titanium suffers from a reduction in its bone integrative properties after sustained exposure to a physiological environment [9]. For these severe conditions, Ti-6Al-4V alloy can be used for orthopedic and dental implants. On the other hand, the elastic modulus of this alloy is much higher than that of cortical bone in addition to the toxicity of V and Al [10]. This weakness phenomenon of pure Titanium was detected also in industrial applications. It has been found that most of the catastrophic failures in most of this material commonly was fatigue and originate at the surface, edges, trailing edges, tips, and roots [11]. To overcome these problems, many surface treatments are applied. The conventional surface hardening (chemical heat treatment) such as nitriding [12], carburizing [13], boriding [14], and thermal spray coatings [15,16] can deform the workpiece and the treatments take long times [17]. Also, limited bond strength between the coating and the substrate is resulted in cases of thermal spray coatings [17].

These problems can be eliminated, and the wear and corrosion resistances of pure titanium can be enhanced by application of laser surface treatments such as melting [18] and cladding [19]. As reported by Pei and Hosson [20], the surface of the specimens treated by laser surface melting is modified mainly by the homogenization and refinement of the microstructure. As a result, the wear, corrosion, and fatigue properties of the parts can be improved. The main advantages of this process over the traditional surface treatments are high cooling rates and low distortion [21]. The high cooling rate can enhance the hardness and ductility for most fine-grained materials when compared to their coarse-grained counterparts [22]. In terms of biocompatibility, as reported in [8], the laser surface melting treatment decreases the contact angle with the human cell and as a result more cell adhesion to the surface. Generally, for pure titanium, the problem of enhancement of their tribological [23,24], mechanical and fatigue [25,26] properties remains the issue of the day [23]. Therefore, the present work has been planned to modify the surface of pure Ti by laser surface melting.

2 Materials and Methods

The surface of commercially pure titanium (CP-Ti) specimens with dimensions of 100 X 60 X 7 mm was modified by laser surface melting using 3 kW single mode fiber laser system (YLS-3000-SM, IPG Photonics) with laser power of 3 kW and Beam diameter of 40 μm. The surfaces of specimens were cleaned, and the oxides were removed by grinding using emery papers. Then, the specimens were washed with alcohol to remove any contaminates. The treatment was carried out at processing powers of 1000, 1500 and 2000 W, and travelling speeds of 4 and 30 mm/s. The focal distances were 24 and 8.5 mm at speeds of 4 and 30 mm/s, respectively. The processing conditions are summarized in Table 1 . The processes were carried out in argon atmosphere. The microstructures of the coated layer and substrates were investigated using optical microscope and scanning electron microscope equipped with EDX analyzer. The micro-Vickers hardness in the treated zone and the substrate were measured with an indentation load of 9.8 N and loading time 15s at room temperature. The wear behaviour of the laser treated zone was evaluated using a pin-on-disk dry sliding wear tester in air at room temperatures. A stationary sample with a diameter of 2.5 mm was slid against a rotating disk with a rotational speed of 265 rpm for 15 min. The tests were carried out at a fixed load of 2 kg applied to the pin. Before the test, all the specimens were ground on emery paper up to # 600 to get smooth and flattened surface. The specimens were weighted before and after the test with a sensitive electronic balance with an accuracy of 0.001 g. The differences in average weight before and after the wear test were measured and accounted. Three specimens of each condition were chosen for wear tests. The untreated base metal was selected as the reference material for the wear test. The corrosion behavior of the substrate and the cladding layer were evaluated by the corrosion current density and the corrosion potential obtained from polarization curves in a 3 wt. % NaCl solution at room temperature with an IM-6 electrochemical workstation. The scanning potential can be in the range of -1.0 to +2 V, and the scanning rate was 5 mV/s.

Table 1. Laser processing conditions

Sample No.	Powers, W	Travelling speed mm/s	Defocusing distance, mm
# 1	2000	4	24
# 2	1500	4	24
# 3	1000	4	24
# 4	1500	30	8.5

3 Results and Discussion

3.1 Macro- and micro-structures analysis

The pure titanium that used as a base metal was consisted of coarse long parallel α-platelets as shown in Figure 1. The optical macrographs of laser treated CP-Ti are shown in Figure 2. Figure 2a, b & c show the macrostructures produced by application of the treatment at fixed travelling speed of 4 mm/s and process powers of 2000, 1500 and 1000 W, respectively. However, Figure 2d represents an example for macrostructure produced at high travelling speed; 30 mm/s and processing power of 1500 W. In all cases, three zones were observed: laser-melted zone (MZ), heat-affected zone (HAZ) and base metal (BM). From these figures, it is clear that, the depths of the resulted zones; melted and solidified and heat affected zone; are affected by the treatment conditions. Generally, the depth of the treated zone was decreased by decreasing the laser powers, as clearly shown in Figure 2(a-c). At laser power of 2000 W, the heat input became very large, and in consequence, the cooling rate became relatively slow which enlarge the depth of the MZ (0.8 mm). When the laser power decreased to 1000 W, the generated heat input was reduced, and the cooling rate become very fast yielding a melted zone of about 0.6 mm depth. The depth of heat affected zone was also increased by the increase of processing power. On the other hand, the widths of the melted and solidified zones were nearly remained constant in these conditions (1000, 1500 and 2000 W with 4 mm/s). By increasing the travelling speed from 4 mm/s to 30 mm/s and decreasing the focusing distance from 24 to 8.5 mm, some changes were noticed in the macrostructure, as shown in Figure 1 d. In this case, the depths, and widths of both melted and heat affected zones were remarkably decreased. The increase of travelling speed decreases the heat input per unit area, and thus, the depth and width of the two zones (MZ and HAZ) are decreased. Also, the decrease of the focusing distance concentrated the heat only on the surface which decreases the width and depth of the melted zone.

The optical and SEM micrographs for the microstructures of the different zones (MZ and HAZ) after application of laser surface melting at fixed travelling speed of 4 mm/s and processing power of 2000 W are shown in Figure 3. The structure of the melted and solidified zone was consisted of α' martensite in its acicular morphology together with coarse plate-like α phase as shown in Figure 3(a-c). The formation of acicular α' martensite may be due to the rapid cooling during solidification. The arms of the acicular α' martensite were relatively thick and short. Regarding the heat affected zone, as shown in Figure 3(d), it was consisted of short α-platelets in addition to some α' martensite. When the processing power was decreased to 1500 W at the same travelling speed of 4 mm/s, the amount of acicular α' martensite was increased with longer length in both melted and heat affected zones as shown in Figure 4. When the processing power was decreased, the cooling rate during solidification became faster, which increase the amount of acicular α' martensite. Figure 5 shows the micrographs for the microstructures of different zones for the specimens treated at processing power of 1000 W and travelling speed of 4 mm/s. More acicular thin and long α' martensite appeared in the melted zone. At the same time, plate-like α phase was detected.

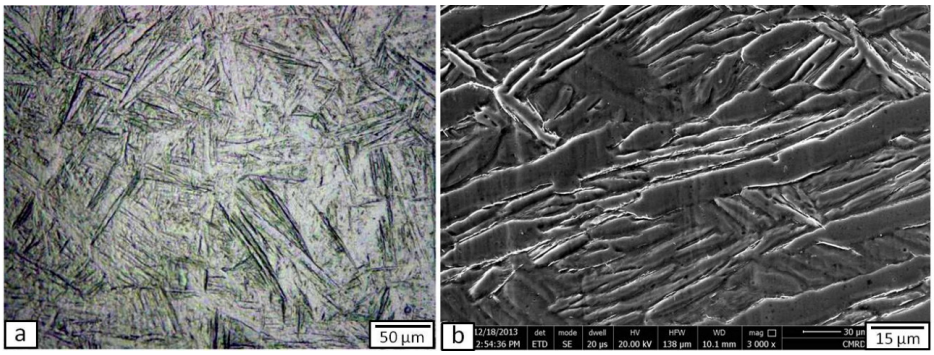

Fig 1. Microstructure of the commercially pure titanium base metal.

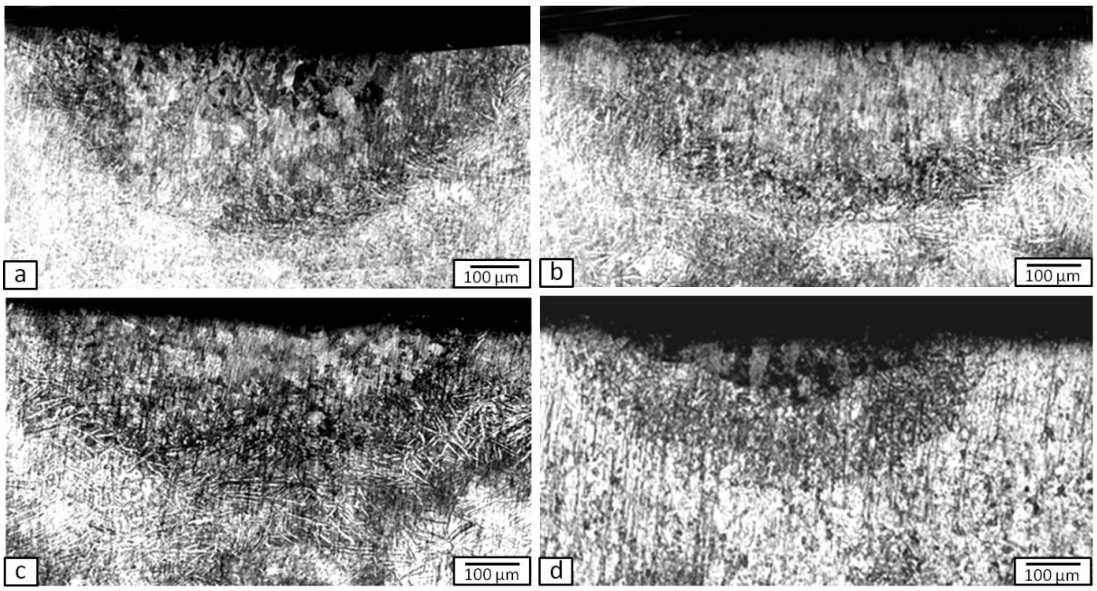

Fig 2. Optical macrographs of the cross-section of the laser treated zone at (a) power of 2000 W and travelling speed of 4 mm/s, (b) power of1500 W and travelling speed of 4 mm/s, (c) power of 1000 W and travelling speed of 4 mm/s, and (d) power of 1500 W, travelling speed of30 mm/s. The defocusing distance was 24 mm at (a-c) and 8.5 mm at (d).

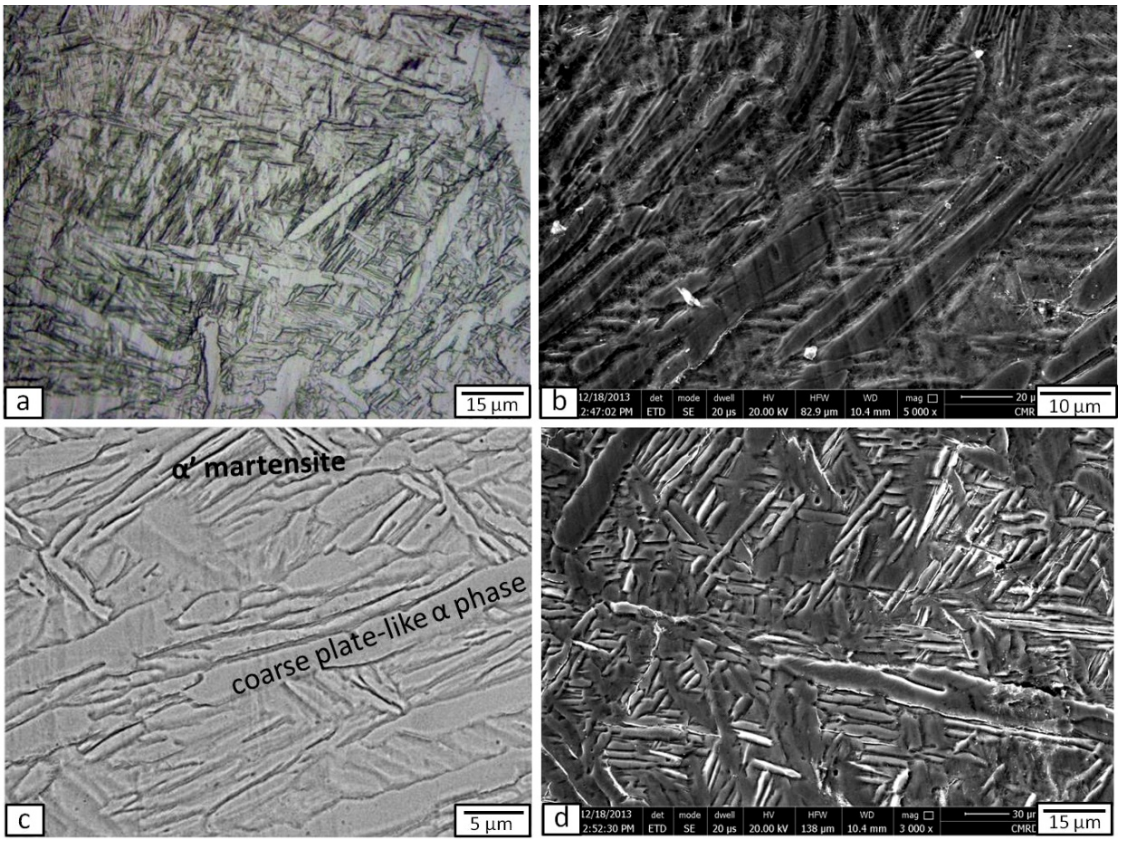

Fig 3. Optical and SEM micrographs of the laser treated zone with processing power of 2000W and travelling speed of 4 mm/s.

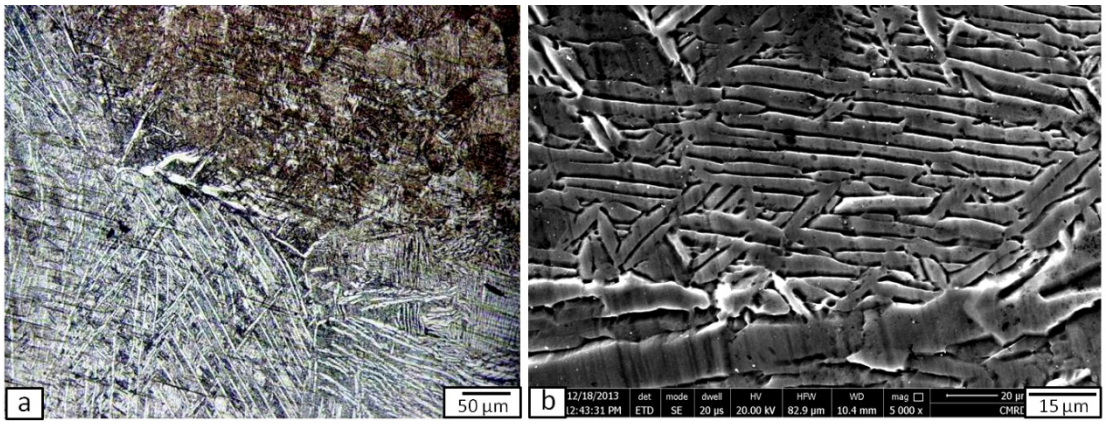

Fig 4. Optical and SEM micrographs of the laser treated zone with processing power of 1500W and travelling speed of 4 mm/s.

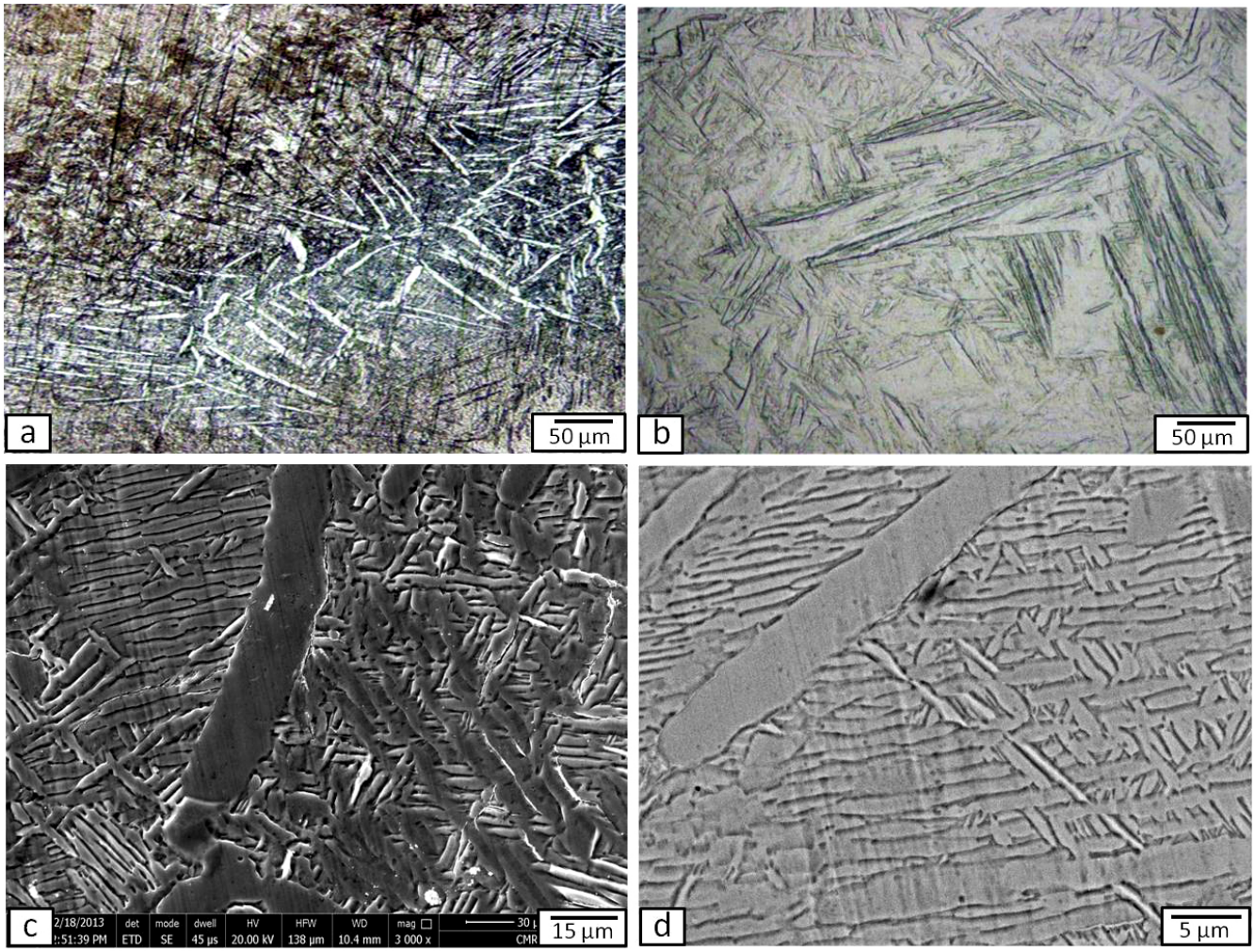

Fig 5. Optical and SEM micrographs of the laser treated zone with processing power of 1000W and travelling speed of 4 mm/s.

To study the effect of extremely higher cooling rate, both the travelling speed and the defocusing distance were changed to be 30 mm/s and 8.5 mm, respectively. Figure 6 shows the microstructures of the melted zone (Figure 6(a)) and the heat affected zone (Figure 6(b)). The melted zone was consisting of very fine acicular α' martensite. This is due to the very rapid cooling rate at this condition. Moreover, the heat affected zone also shows fine α' martensite.

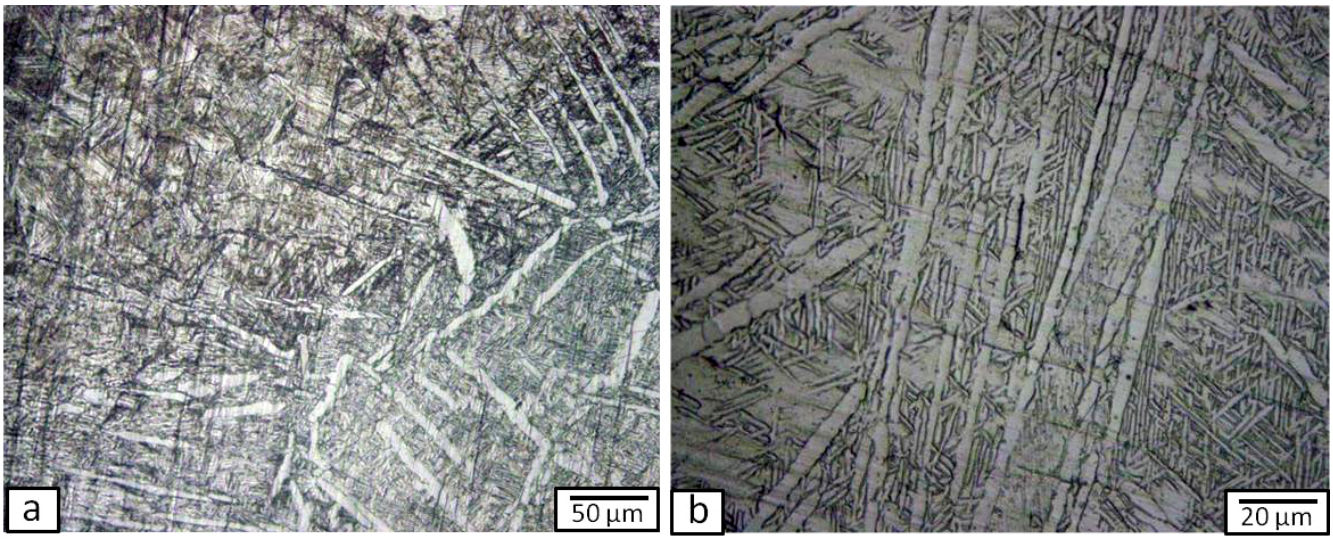

Fig 6. Optical micrographs of the laser treated zone with processing power of 1500 W, travelling speed of 30 mm/s, and defocusing distance of 8.5 mm, where (a) melted zone and (b) heat affected zone.

3.2 Surface and subsurface layer microhardness evaluation

The microhardness on the top surface and the cross-sectional region of the CP-Ti in the as-received condition and after laser surface melting has been taken for the Vickers load of 9.8 N and loading time of 15 Sec. The average value of hardness for the untreated base material is about 275 HV. Figure 7 shows the variation of microhardness for the laser treated samples at different processing powers; 2000, 1500 and 1000 W; and fixed travelling speed; 4 mm/s. Also, the hardness of the high travelling speed (30 mm/s) sample is also demonstrated. As it can be seen, the hardness showed higher values at the melted and solidified zones. This enhancement of hardness can be mainly ascribed to the change of α phase to "acicular" martensite α' structure and grain refinement. The rapid cooling after laser surface melting (up to $10^{6\,\circ}$ K/s [27]) leads to formation of meta-stable structure with fine structure which improves the hardness. In all cases of the present study, refined structures with modified martensitic structure resulted in the melted and solidified zone due to the application of the laser surface melting treatment. The power of the laser beam is one of the main factors in laser surface melting (LSM) which alter the depth and width of melted and heat affected zones to obtain desired surface properties. The hardness values near the free surface treated with low power; 1000 W; are higher than those in the two other cases; 1500 and 2000 W. For example, the hardness reached to 445 HV in case of 1000 W, while it reached to 400 HV in case of 2000 W. On the other hand, the laser power has a straight effect on the depth of the hardened zone. As the laser power is increases, the higher hardness appeared to a deeper depth inside the materials (Compare the plot of hardness for 2000 W and that of 1000 W). Regarding the hardness of the sample treated at fast travelling speed (30 mm/s) with a defocusing distance of 8.5 mm, it shows a higher value (it reaches 710 HV) but within a shallow depth.

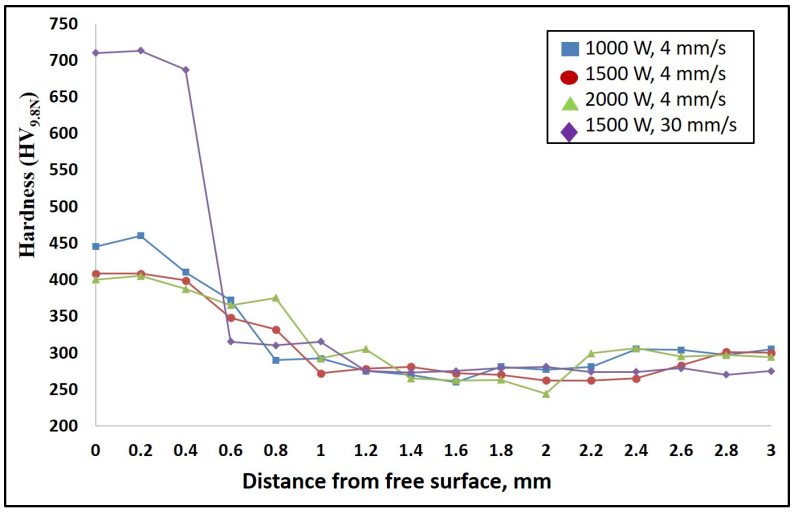

Fig 7. Hardness distribution along the depth of laser treated zone with different processing powers and travelling speeds.

3.3 Wear resistance evaluation

The wear resistance of the laser treated surfaces together with the un-treated CP-Ti surface was investigated through pin-on-disk dry sliding wear test and the results were summarized in terms of weight losses in Figure 8. It is clear from this figure that the laser treatment with all processed condition is remarkably increased the wear resistance of the CP-Ti. The weight loss of the un-treated substrate was almost twice of even the softer treated condition (2000 W). This is due to the faster cooling rate of the laser surface technology which melted a thin layer of the surface and then allowed it to be solidified in a very short time. This fast cooling is an optimum chance to form the hard martensite structure. This martensitic structure strengthens the surface and resist the materials removal during the wear test and inconsequence the field wear conditions. When the processing power decreased at fixed travelling speed, the heat input deceased, and the cooling rate increased. This increment in the cooling rate produce more finer martensite structure in the surface which directly affect the wear resistance (lower materials weight loss) as clearly shown in the step column in Fig. 8. The weight losses of 1000 W sample was almost half of that of 2000 W. Increasing the travelling speed to 30 mm/s accelerate the cooling rate and it directly reduce the wight loss to almost 0.5 gm.

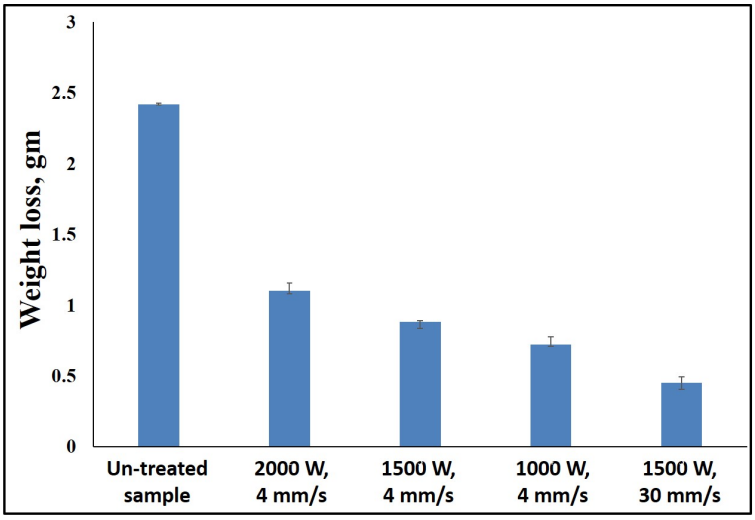

Fig 8. Wear weight losses of the laser treated surfaces at different processing powers and travelling speeds together with the un-treated CP-Ti alloy.

3.4 Corrosion resistance evaluation

For simply corrosion resistance evaluation, one of the laser-treated sample (1000 W) was compared with the un-treated CP-Ti through polarization curves and the results were shown in Figure 9. By comparing the curves of Figure 9(a) with 9 (b), the corrosion potential (X-axis) shows more negative values for the un-treated sample (a), while it shows more positive values for the laser treated sample (Figure 9(b). At the same time, the Y-axis of the corrosion current shows more negative values for the laser treated sample compared to the un-treated sample. As stated in many works [28–30], when the corrosion potential shifts to more positive values, the polarization resistance increase. Also, when the current density decrease, the corrosion resistance increase. The resulted finer microstructure of the laser treated surface has a strong influence on chemical stability and it enhances the corrosion resistance.

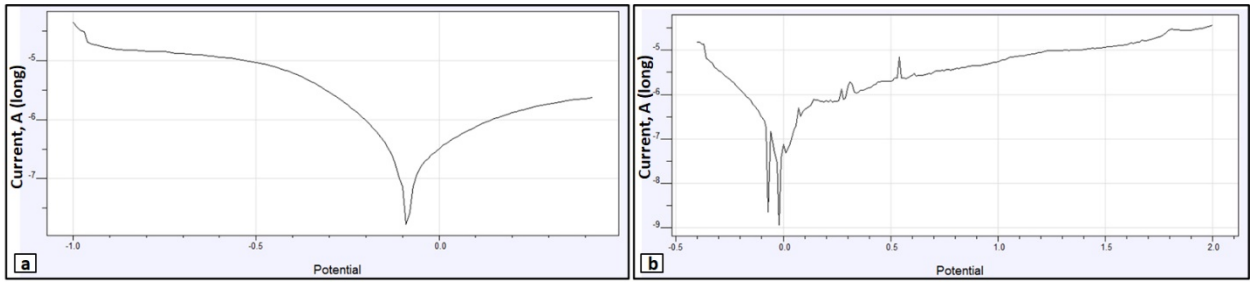

Fig 9. Polarization curves of the un-treated CP-Ti substrate (a), and the laser treated sample produced at processing power of 1000 W and travelling speed of 4 mm/s.

4 Conclusion

The surface of commercially pure titanium (CP Ti) was treated by laser melting in argon atmosphere at different processing powers (2000, 1500 and 1000W) and travelling speeds of 4 and 30 mm/s. The treated specimens were investigated in macro and microscopically scale using optical and scanning electron microscopes. Microhardness measurements were also carried out through the thickness of the laser treated zones. Wear and corrosion resistances of the treated zones were evaluated. The results of this work led to the following conclusions:

- The laser treated areas with all applied conditions resulted in sound melted and solidified zone on the surface of the commercially pure titanium without any noticeable defects.
- The increase of the processing power and/or decrease of the travelling speed cause increases in the depth of the melted and heat affected zones.
- Acicular martensite α' structure was observed within the melted and solidified zone in all experimental conditions. The amount of this acicular martensite α' structure was increased and its depth was decreased by decreasing the processing power.
- The surface hardness of the CP-Ti sample was improved of 62% when treated at processing power of 1000 W and travelling speed of 4 mm/s. As the processing power was increased, the hardness improvement was decreased.
- The wear and corrosion resistances were remarkably improved by application of laser surface melting.

Acknowledgement

The authors would like to express their appreciation for the support provided by the Scientific Research Deanship, Islamic University of Madinah, with Tamayyuz grant number 7/40.

References

1) de Mello MG, Salvador CAF, Fanton L, Caram R. High strength biomedical Ti–13Mo–6Sn alloy: Processing routes, microstructural evolution and mechanical behavior. *Materials Science and Engineering: A*. 2019;764. Available from: https://dx.doi.org/10.1016/j.msea.2019.138190.
2) Fayomi J, Popoola API, Popoola OM. Corrosion performances and thermal behavior of AA8011 reinforced with hybrid-nano ZrB2 + Si3N4 particulates for automobile applications. *Materials Research Express*. 2019;6. Available from: https://dx.doi.org/10.1088/2053-1591/ab4fd0.
3) Zimmermann S, Specht U, Spieß L, Romanus H, Krischok S, Himmerlich M, et al. Improved adhesion at titanium surfaces via laser-induced surface oxidation and roughening. *Materials Science and Engineering: A*. 2012;558:755–760. Available from: https://dx.doi.org/10.1016/j.msea.2012.08.101.

4) Karre R, Dey SR. Progress in Development of Beta Titanium Alloys for Biomedical Applications. Reference Module in Materials Science and Materials Engineering. 2019. Available from: https://doi.org/10.1016/B978-0-12-803581-8.10501-6.
5) Quazi MM, Ishak M, Fazal MA, Arslan A, Rubaiee S, Qaban A, et al. Current research and development status of dissimilar materials laser welding of titanium and its alloys. *Optics & Laser Technology*. 2020;126. Available from: https://dx.doi.org/10.1016/j.optlastec.2020.106090.
6) Koizumi H, Takeuchi Y, Imai H, Kawai T, Yoneyama T. Application of titanium and titanium alloys to fixed dental prostheses. *Journal of Prosthodontic Research*. 2019;63(3):266–270. Available from: https://dx.doi.org/10.1016/j.jpor.2019.04.011.
7) Xuanyong L, Chu PK, Chuanxian D. Surface modification of titanium, titanium alloys, and related materials for biomedical applications. *Materials Science and Engineering: R*. 2014;47:49–121. Available from: https://doi.org/10.1016/j.mser.2004.11.001.
8) Li JPSH, Blitterswijk CAV. Cancellous Bone from Porous TI6Al4V by Multiple Coating Technique. *Journal of Materials Science: Materials in Medicine*. 2016;17:179–185.
9) Mitsuo N. Mechanical biocompatibilities of titanium alloys for biomedical applications. *Journal of the Mechanical Behavior of Biomedical Materials*. 2018;1:30–42. Available from: https://doi.org/10.1016/j.jmbbm.2007.07.001.
10) Dinda GP, Shin J, Mazumder J. Pulsed laser deposition of hydroxyapatite thin films on Ti-6Al-4V: Effect of heat treatment on structure and properties. *Acta Biomaterialia*. 2019;5:1821–1830. Available from: https://doi.org/10.1016/j.actbio.2009.01.027.
11) Sallica-Leva E, Jardini AL, Fogagnolo JB. Microstructure and mechanical behavior of porous Ti–6Al–4V parts obtained by selective laser melting. *Journal of the Mechanical Behavior of Biomedical Materials*. 2013;26:98–108. Available from: https://dx.doi.org/10.1016/j.jmbbm.2013.05.011.
12) Shen H, Wang L. Formation, tribological and corrosion properties of thicker Ti-N layer produced by plasma nitriding of titanium in a N2-NH3 mixture gas. *Surface and Coatings Technology*. 2020;393. Available from: https://doi.org/10.1016/j.surfcoat.2020.125846.
13) Semboshi S, Iwase A, Takasugi T. Surface hardening of age-hardenable Cu–Ti alloy by plasma carburization. *Surface and Coatings Technology*. 2015;283:262–267. Available from: https://dx.doi.org/10.1016/j.surfcoat.2015.11.003.
14) Sireli GK, Bora AS, Timur S. Evaluating the mechanical behavior of electrochemically borided low-carbon steel. *Surface and Coatings Technology*. 2020;381. Available from: https://dx.doi.org/10.1016/j.surfcoat.2019.125177.
15) Hoshiyama Y, Miyazaki T, Miyake H. Zirconium carbide dispersed high Cr–Ni cast iron produced by plasma spraying. *Surface and Coatings Technology*. 2013;228:S7–S10. Available from: https://dx.doi.org/10.1016/j.surfcoat.2012.10.019.
16) Li W, Cao C, Yin S. Solid-state cold spraying of Ti and its alloys: A literature review. *Progress in Materials Science*. 2020;110:100633–100633. Available from: https://dx.doi.org/10.1016/j.pmatsci.2019.100633.
17) Suhaimi MA, Yang GD, Park KH, Hisam MJ, Sharif S, Kim DW. Effect of Cryogenic Machining for Titanium Alloy Based on Indirect, Internal and External Spray System. *Procedia Manufacturing*. 2018;17:158–165. Available from: https://dx.doi.org/10.1016/j.promfg.2018.10.031.
18) Yadroitsev I, Krakhmalev P, Yadroitsava I. Selective laser melting of Ti6Al4V alloy for biomedical applications: Temperature monitoring and microstructural evolution. *Journal of Alloys and Compounds*. 2014;583:404–409. Available from: https://dx.doi.org/10.1016/j.jallcom.2013.08.183.
19) Kanyane LR, Adesina OS, Popoola API, Farotade GA, Malatji N. Microstructural evolution and corrosion properties of laser clad Ti-Ni on titanium alloy (Ti6Al4V). 2019.
20) Pei YT, Hosson JD, Th. Producing Functionally Graded Coatings by Laser- Powder cladding. *JOM-e*. 2002;51(1):1–5. Available from: http://www.tms.org/pubs/journals/JOM/0001/Pei-000.htm1.
21) Zhu Z, Li J, Peng Y, Shen G. In-situ synthesized novel eyeball-like Al2O3/TiC composite ceramics reinforced Fe-based alloy coating produced by laser cladding. *Surface and Coatings Technology*. 2020;391. Available from: https://doi.org/10.1016/j.surfcoat.2020.125671.
22) Mohseni E, Zalnezhad E, Bushroa AR. Comparative investigation on the adhesion of hydroxyapatite coating on Ti–6Al–4V implant: A review paper. *International Journal of Adhesion and Adhesives*. 2014;48:238–257. Available from: https://dx.doi.org/10.1016/j.ijadhadh.2013.09.030.
23) Lin Y, Yao J, Lei Y, Fu H, Wang L. Microstructure and properties of TiB 2 –TiB reinforced titanium matrix composite coating by laser cladding. *Optics and Lasers in Engineering*. 2016;86:216–227. Available from: https://dx.doi.org/10.1016/j.optlaseng.2016.06.013.
24) Huang S, Agyenim-Boateng E, Sheng J, Yuan G, Dai FZ, Ma DH, et al. Effects of laser peening with different laser power densities on the mechanical properties of hydrogenated TC4 titanium alloy. *International Journal of Hydrogen Energy*. 2019;44(31):17114–17126. Available from: https://dx.doi.org/10.1016/j.ijhydene.2019.05.002.
25) du Plooy R, Akinlabi ET. Analysis of laser cladding of Titanium alloy. *Materials Today: Proceedings*. 2018;5(9):19594–19603. Available from: https://dx.doi.org/10.1016/j.matpr.2018.06.322.
26) Pascu A, Rosca JM, Stanciu EM. Laser cladding: from experimental research to industrial applications. *Materials Today: Proceedings*. 2019;19:1059–1065. Available from: https://dx.doi.org/10.1016/j.matpr.2019.08.021.
27) Kusiński J, Ciaś A, Pieczonka TM, Smith AB, Rakowska A. Wear properties of T15 PM HSS made indexable inserts after laser surface melting. *Journal of Materials Processing Technology*. 1997;64(1-3):239–246. Available from: https://dx.doi.org/10.1016/s0924-0136(96)02573-3.
28) El-Labban HF, Mahmoud ERI, Algahtani A. Microstructure, Wear, and Corrosion Characteristics of TiC-Laser Surface Cladding on Low-Carbon Steel. *Metallurgical and Materials Transactions B*. 2016;47(2):974–982. Available from: https://dx.doi.org/10.1007/s11663-016-0602-4.
29) Fayomi OSI, Popoola API. Aigbodion V.S. Investigation on microstructural, anti-corrosion and mechanical properties of doped Zn-Al-SnO2 metal matrix composite coating on mild steel. *Journal of Alloys and Compounds*. 2015;623:328–334.
30) Xu WF, Jun MA, Wang M, Lu HJ. Yu-xuan Luo Effect of cooling conditions on corrosion resistance of friction stir welded 2219-T62 aluminum alloy thick plate joint. *Transactions of Nonferrous Metals Society of China*. 2020;30(6):1491–1499. Available from: https://doi.org/10.1016/S1003-6326(20)65313-4.